Geo-Mar Lett (2012) 32:289–300
DOI 10.1007/s00367-011-0268-5

ORIGINAL

Selective geochemistry of iron in mangrove soils in a semiarid tropical climate: effects of the burrowing activity of the crabs *Ucides cordatus* and *Uca maracoani*

J. M. C. Araújo Jr. · X. L. Otero · A. G. B. Marques · G. N. Nóbrega · J. R. F. Silva · T. O. Ferreira

Received: 19 May 2011 / Accepted: 21 November 2011 / Published online: 14 December 2011

Abstract Bioturbation by crabs may affect processes associated with organic matter decomposition in mangrove soils. This study examines how two crabs (*Uca maracoani* and *Ucides cordatus*), which are of substantial ecological and economic importance in semiarid coastal areas of Brazil, affect biogeochemical processes in mangrove soils. For this purpose, the physicochemical and geochemical parameters of the soils at different sites were analyzed. The redox potential was always positive at bioturbated sites (+12 to +218 mV), indicating more oxidizing conditions conducive to the oxidation of pyrite and precipitation of oxyhydroxides. In contrast, anoxic conditions prevailed at the control site (Eh<0 mV), and the most abundant form of iron was Fe-pyrite. The highest degree of iron pyritization (DOP) was observed in soils from the control site (~48%) and the lowest in the bioturbated soils (5–16%), indicating that crabs have an oxidative effect on iron sulfides. The results also suggest that *U. cordatus* has a higher oxidizing capacity than *U. maracoani*, probably because it constructs larger and deeper burrows. The results demonstrate that both crabs must be considered as important bioturbators in Brazilian semiarid mangrove soils, being capable of enhancing organic matter decomposition and also shifting the dominant pathway of organic matter degradation.

J. M. C. Araújo Jr. · A. G. B. Marques · G. N. Nóbrega · T. O. Ferreira (✉)
Departamento de Ciências do Solo,
Universidade Federal do Ceará, UFC,
M.B. 12168 Fortaleza, Ceará, Brazil
e-mail: tiago@ufc.br

X. L. Otero
Departamento Edafoloxía e Química Agrícola, Facultade de Bioloxía, Universidade de Santiago de Compostela,
15782 Santiago de Compostela, Spain

J. R. F. Silva
Departamento de Biologia, Universidade Federal do Ceará, UFC,
CEP 60457-970 Fortaleza, Ceará, Brazil

Introduction

Mangrove forests are highly productive environments and are of substantial ecological importance and conservation value, because they function as nursery sites for several fresh and salt water species (Walters et al. 2008). They also play an important role in protecting coastal areas from chronic disturbances such as tsunamis and shoreline erosion (Kathiresan and Rajendran 2005; Alongi 2008). These environments are characterized by saline soils, which have high organic matter contents and are subject to prolonged periods of water saturation (Clough 1992). Such conditions lead to the depletion of molecular oxygen, the diffusion of which is limited in aqueous media, causing organic matter decomposition to occur via anaerobic pathways and, therefore, at the expense of electron acceptors other than O_2 (NO_3^{2-}, Mn (IV), Fe(III), SO_4^{2-}; Ponnamperuma 1972; Neue et al. 1997; Seybold et al. 2002).

Because of the high sulfate concentrations in seawater, high organic matter content, and reactive iron derived from active hydrological systems (rivers and tides), the decomposition of organic matter in mangrove environments is mainly ascribed to sulfate reduction, which results in pyrite formation (Alongi et al. 1996). The solid-phase sulfides produced during sulfate reduction (acid volatile sulfides, and pyrite) have been extensively studied because of their ability to act as sinks for heavy metals (e.g., Huerta-Díaz and Morse 1992; Otero and Macías 2002a, 2003; Machado et al. 2004). However, the redox conditions of mangrove

soils may vary in response to a variety of biotic and abiotic factors (e.g., Ferreira et al. 2010), and thereby alter the mobilization and bioavailability of trace metals at impacted sites (e.g., Morse 1994; Machado et al. 2002, 2004).

Previous studies have shown that different respiration processes may play an important role in the mineralization of organic matter, including aerobic (Alongi et al. 2001) and suboxic respiration (Kristensen et al. 2000, 2010) that, in some cases, may predominate over sulfate reduction (Gribsholt et al. 2003). The occurrence or the dominance of a given pathway may vary due to seasonal changes in rainfall (Marchand et al. 2004; Ferreira et al. 2007a), in function of physiographic characteristics (Ferreira et al. 2007b), plant activity (Gleason et al. 2003; Marchand et al. 2004; Otero et al. 2006), and local microtopography (Ferreira et al. 2010).

In this context, some recent studies have indicated that a shift toward respiratory processes other than sulfate reduction may arise as a result of the activity of the macrobenthic community (Kristensen et al. 2000; Nielsen et al. 2003; Kristensen and Alongi 2006; Kristensen 2008; Ferreira et al. 2007a; Ferreira 2010; Penha-Lopes et al. 2010). Because bioturbation by crabs involves the reworking of soil during the search for food and the construction of channels at low tide (Perillo et al. 2005), it increases the diffusive transport of gases to the substrate (Kristensen et al. 2010), thereby favoring its oxidation. Bioturbation also enables the transport of non-decomposed organic matter and oxidizing compounds to subsurface layers (Kostka et al. 2002), resulting in oxidized layers and/or oxidized micro-sites in the subsurface layer as a result of the distribution of the channels. According to Kristensen et al. (2010), in mangrove substrates with high crab activity, iron reduction may become the dominant anaerobic respiratory pathway because the availability of reactive iron is determined by the oxidizing capacity of the crab burrows.

The family Ocypodidae, which includes the genera *Uca* and *Ucides*, is considered of substantial ecological (Schories et al. 2003; Nordhaus et al. 2006) and economic importance (Glaser and Diele 2004; Diele et al. 2005) in estuarine environments of Brazil. The fiddler crab *Uca maracoani* makes simple, unbranched and relatively shallow burrows (approx. 40 cm deep) that may be shared (Lim 2006; Kristensen 2008). *Ucides cordatus*, in contrast, builds more complex burrows, often with multiple entrances (Bright and Hogue 1972) and with depths between 20 cm and 2 m, which are relatively straight and uniform in aspect (Castilho-Westphal et al. 2008).

As the two crabs differ in, for example, size, feeding habit, reproduction, and also their burrowing activity, they are expected to affect substrate biogeochemistry in different ways. However, very few comparative studies have explored the effects of specific crab species on the composition of mangrove soils, one exception being that of Botto and Iribarne (2000). To our knowledge, no studies have yet addressed the impact of different crab species on mangrove soil geochemistry, especially those soils affected by shrimp aquaculture. Moreover, unlike most tropical mangroves, semiarid mangroves are subject to low rainfall, relatively high temperatures and evaporation rates, and occasional hypersaline conditions. The burrowing activity of crabs may vary strongly under such conditions—temperature and salinity are considered key ecological factors in determining the behavior, survival, development, and growth of crabs (Rome et al. 2005; Diele and Simith 2006; Bianchini et al. 2008).

The objective of the present study was to assess the role of different crabs of the family Ocypodidae (*U. cordatus* and *U. maracoani*) as drivers of some main biogeochemical processes in semiarid Brazilian mangrove soils, in order to improve our understanding of these endangered ecosystems and thereby promote better management and conservation strategies.

Materials and methods

Site description

The mangrove forest of this study is found along the estuary of the Jaguaribe River in the state of Ceará (Aracati County) on the northeast coast of Brazil (Fig. 1). The river basin stretches over 75,669 km^2 between 4–7°S and 37–41°W, and can be subdivided into three major sections: the higher, middle and lower Jaguaribe sub-basins. The study area is located in the lower sub-basin, close to the Aracati County border.

The Jaguaribe River and its tributaries drain an area dominated by Caatinga (a seasonal xerophilous thorn woodland) as the main vegetation unit. The climate in the region is hot and semiarid, being classified as Aw' according to the Köppen climate classification scheme (Kottek et al. 2006; Peel et al. 2007). Climate records from the last 30 years show the mean annual precipitation to be 770 mm and the mean annual temperature 28.5°C. Harsh droughts, generally associated with the El Niño-Southern Oscillation, are common. Furthermore, the extremely high evaporation rate exceeds 10 mm per day (Folhes et al. 2009). In the estuarine zone itself, the mean annual precipitation is 982.6 mm, with most of the rainfall occurring between February and May, whereas the mean annual temperature varies in the range 26–28°C.

The estuary of the Jaguaribe River is marked by the presence of mangroves at different stages of development and regeneration, mainly due to impacts associated with shrimp aquaculture. *Rhizophora mangle*, *Laguncularia racemosa*,

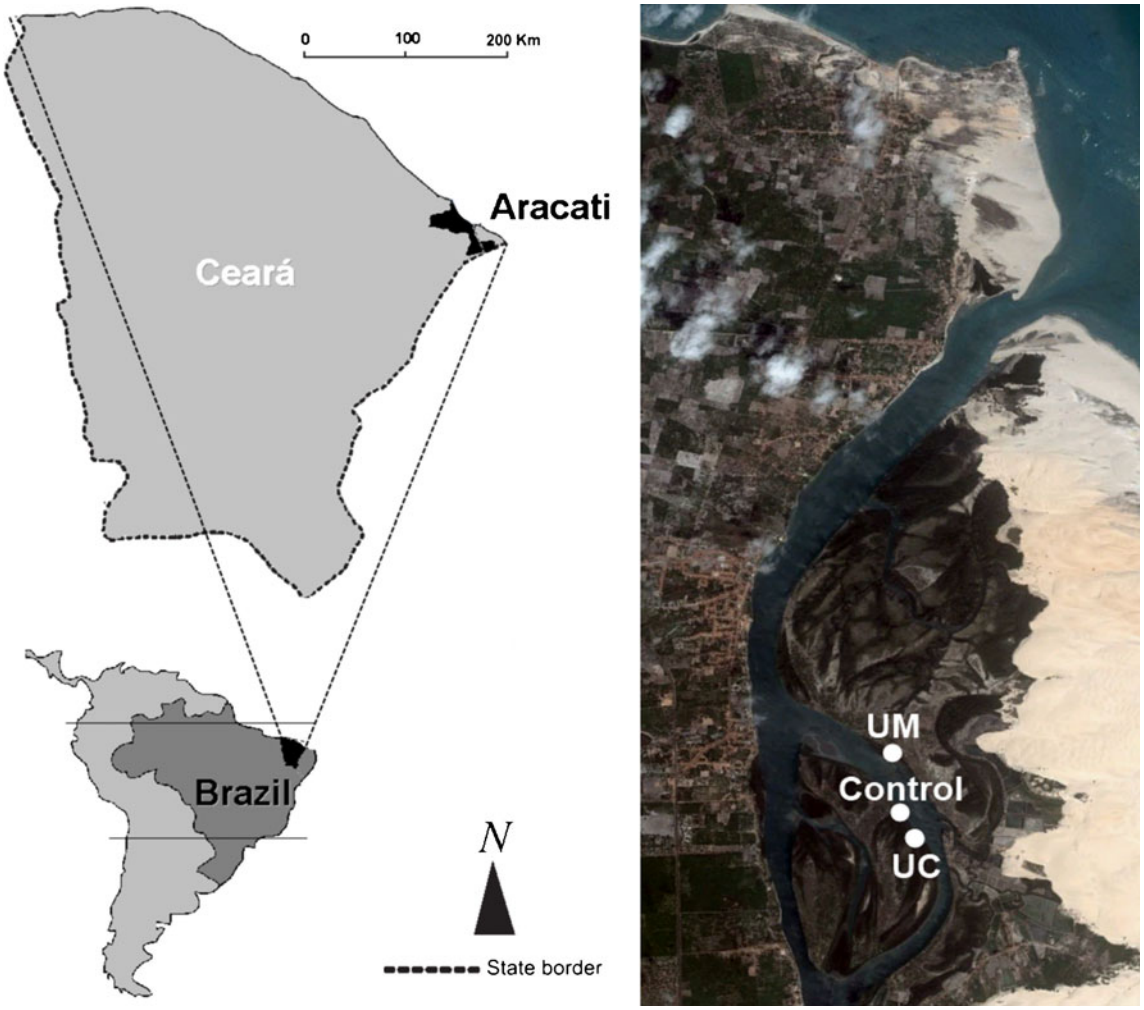

Fig. 1 Map showing the location of the study area along the northeast coast of the state of Ceará, Brazil, and an aerial photograph of the Jaguaribe River estuary indicating the location of the sampling sites: *UC* site populated by *Ucides cordatus*, *UM* site populated by *Uca maracoani*, control site

and *Avicennia schaueriana* are the dominant mangrove species (Tanaka and Maia 2006). All studied soils can be classified as 'sulfaquents' according to the Soil Survey Staff (2010), corresponding to the 'thionic gleysols' of the FAO-World Reference Base (FAO 2006).

Sampling procedures

Sampling sites were located in areas exclusively occupied by a single crab species at high population density (*Ucides cordatus* and *Uca maracoani*; Fig. 2), at similar physiographic

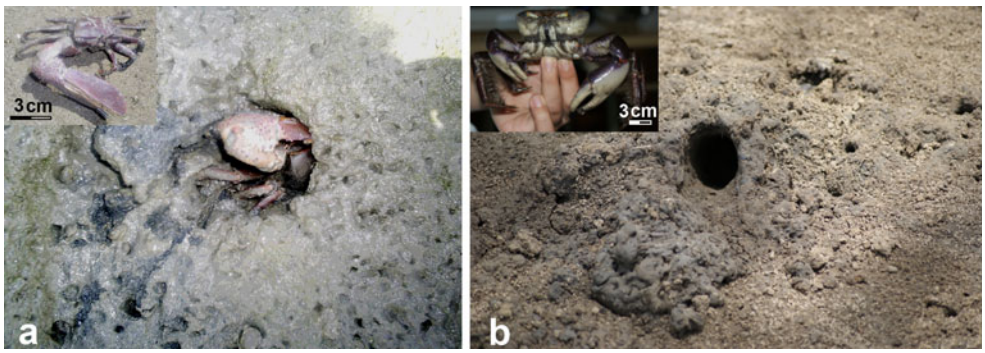

Fig. 2 Photographs of the burrows of **a** *Ucides cordatus*, and **b** *Uca maracoani*, as well as close-ups of the two burrowing crabs (photographs by J.M.C. Araújo Jr.)

positions and without any significant elevation difference. In addition, a control plot was established by fencing off the substrate with nylon nets (1 cm mesh, 1 m in height, and buried to a depth of 1.5 m) to eliminate crab burrowing activity. Before sampling, the control plot was maintained isolated for 3 months. The area of both the sampling and exclusion plots (fenced off) was 1 m^2, the plots being located close to each other to avoid spatial variations. All plots were selected so as to avoid interference from plant activity (absence of pneumatophores, prop roots, and also mangrove plantlets). The control plot and substrates dominated by *U. cordatus* (UC) and *U. maracoani* (UM) were sampled at low tide in May 2009 (i.e., during the rainy season).

In each bioturbated plot, the density of burrows was determined by counting burrow entrances and measuring their depth by carefully inserting a soft rubber wire. At all sites, samples were randomly collected with PVC tubes (50 mm in diameter and 50 cm in length) attached to a soil auger. Six cores were collected within each plot. The tubes were hermetically sealed, maintained at approx. 4°C, and transported upright to the laboratory. The redox potential (Eh) and pH were measured in situ after letting the cores and electrodes equilibrate for approx. 2 minutes. The Eh electrode was checked against a standard Metrohm redox solution at a potential of 250±5 mV and a temperature of 20°C. Probes were inserted in the center of each core collected with the semi-opened cylindrical auger to avoid contact with the atmosphere. The pH was measured with a glass electrode (model MP120; Mettler Toledo) calibrated with pH 4.0 and 7.0 standards, while the redox potentials (Eh) were measured with an oxidation–reduction potential (ORP) platinum electrode. Final readings were corrected by adding the potential (+244 mV) of a calomel reference electrode.

In the laboratory, three cores from each plot were cut into narrow sections (0–3, 3–6, 6–10, 10–15, 15–20, 20–25, 25–30, 30–35, and 35–40 cm) to aid assessment of depth-related variations. The other three cores were sectioned at larger intervals (0–10, 10–20, 20–30, and 30–40 cm) to facilitate a more general comparison between sites and layers.

Analytical procedures

Partitioning of solid-phase Fe was determined by the combined methods of sequential extraction proposed by Tessier et al. (1979), Fortín et al. (1993), and Huerta-Díaz and Morse (1990); for more details, see Ferreira et al. (2007b), and Otero et al. (2009). The procedure enables the recognition of six operationally derived iron pools, which are defined as follows:

- F1, exchangeable iron: extracted with 30 ml of a 1 M $MgCl_2$ solution at pH 7.0; samples were shaken for 30 minutes and centrifuged at 10,000 rpm (4°C) for 30 minutes;
- F2, carbonate-associated iron: extracted with 30 ml of a 1 M NaOAc solution at pH 5.0; samples were shaken for 5 h and centrifuged at 10,000 rpm (4°C) for 30 minutes;
- F3, ferrihydrite iron: extracted with 30 ml of a solution of 0.04 M hydroxylamine + acetic acid 25% (v/v); samples were shaken for 6 h at 30°C and centrifuged at 10,000 rpm (4°C) for 30 minutes;
- F4, lepidocrocite iron: extracted with 30 ml of a solution of 0.04 M hydroxylamine + acetic acid 25% (v/v); samples were shaken for 6 h at 96°C and centrifuged at 10,000 rpm (4°C) for 30 minutes;
- F5, crystalline oxides and iron oxyhydroxides (goethite, hematite): extracted with 20 ml of a solution of 0.25 M sodium citrate + 0.11 M sodium bicarbonate, with 3 g sodium dithionite; samples were shaken for 30 minutes at 75°C and centrifuged at 10,000 rpm (4°C) for 30 minutes;
- F6, Fe-pyrite: extracted with 10 ml concentrated HNO_3; samples were shaken for 2 h at room temperature, and then washed with 15 ml ultra-pure water. Before the extraction of Fe-pyrite, samples were subjected to treatment with 10 M HF for 16 h under agitation to eliminate phylosilicate Fe, and concentrated H_2SO_4 was then added to eliminate Fe associated with organic matter (Huerta-Díaz and Morse 1990, 1992).

Between each step of the extraction procedure, samples were washed with 20 ml ultra-pure water. The degree of iron pyritization (DOP) was calculated as follows:

$$\mathrm{DOP}(\%) = [(\text{pyrite Fe})/(\text{reactive Fe} + \text{pyrite Fe})] \times 100$$

The DOP determines the percentage of reactive iron incorporated in the pyritic fraction (Berner 1970), and enables comparison between soils with different reactive iron contents. We calculated the DOP by considering reactive iron (iron that can react with sulfide to form pyrite) as $\sum F1 \rightarrow F5$ (Otero and Macías 2002a). It is emphasized that, although most sequential extraction procedures are not fully selective, this approach remains useful in evaluating the availability and mobility of metals in solid phase (e.g., Hullebusch et al. 2005; Bacon and Davidson 2008; Claff et al. 2010).

Subsamples were taken from the middle of each soil sample and placed in 50-ml polypropylene bottles, which were sealed hermetically before being centrifuged at 10,000 rpm for 30 minutes at 4°C for pore water extraction (Otero and Macías 2002a). One subsample of pore water was analyzed for sulfate and chloride by standard soil procedures, using titration with $AgNO_3$ (0.05 N) to determine

Cl^-, and $BaCl_2$ (10%) to precipitate SO_4^{2-}, which is then quantified by gravimetry (EMBRAPA 1997). Another subsample of pore water was used for salinity measurements with a handheld refractometer.

Total organic carbon (TOC), total N (TN) and total S (TS) were determined by an elemental analyzer (LECO CNS, model 2000). For TOC quantification, subsamples were pretreated with 6 N HCl to remove inorganic carbon, while TN and TS were quantified in untreated subsamples. The hydrometer method (Gee and Bauder 1986) was used for particle-size analysis, preceded by oxidation of organic matter with H_2O_2 by using a combination of physical (overnight shaking) and chemical (0.015 M $(NaPO_3)_6$+1.0 M NaOH) dispersal methods. The classification of granulometric composition follows the ternary scheme proposed by Flemming (2000).

Statistical analysis

The differences between plots were established by Student t test with 95% confidence intervals, using the samples with the lower depth resolution (0–10, 10–20, 20–30, and 30–40 cm) to describe statistical differences between the study sites. In the corresponding diagrams, the bars marked with different letters indicate significant differences at $p<0.05$. The relationships between different variables were determined by calculating Spearman's coefficients of correlation (r_s) with the same depth resolution. All statistical analyses were carried out with the SigmaStat 3.1 computer software (Systat 2008).

Results

Density and depth of burrows

The mean burrow density at the UC site was 12±3 m^{-2}, whereas at the UM site it was 58±12 m^{-2}. The depths of burrows varied between 50 and 100 cm at the UC site, and between 20 and 40 cm at the UM site.

General characterization of the soils

The particle-size distributions reveal substantial differences between sites inhabited by *U. cordatus* and *U. maracoani* (Table 1), the UM site being characterized by a coarser texture. Overall, sand was the dominant size fraction at UM (min. 55%, max. 83%), whereas silt was dominant at UC (min. 46%, max. 55%). The sediment composition at the control plot occupied an intermediate position (Fig. 3).

TOC contents vary little between the bioturbated sites (Table 1), the highest percentages usually being found in the uppermost layers characterized by the highest mud contents (UC: 0.7–1.4%; UM: 1.3–1.7%). The TOC contents in samples from the control site are higher than those from both bioturbated sites, the values ranging from 1.58 to 2.91%. Total N follows the same pattern as observed for TOC, with the highest values in the surface layers of the control site (Table 1). Total S contents differ strongly between non-bioturbated and bioturbated sites. In soils from the bioturbated sites, the total S values vary from 0.15–0.18% at the UC site to 0.40–0.46% at the UM site, whereas

Table 1 Total contents of sand, silt, clay, organic carbon (TOC), S, and N in the soils of the three study sites, as well as pore water salinities and molar ratios of $SO_4^{=}/Cl^-$ at the UC and UM sites. Normalization of the concentration of $SO_4^{=}$ to Cl^- shows that $SO_4^{=}$ variations were not due to changes in salinity, but rather to sulfate reduction (*n.d.* no data)

Depth (cm)	Clay (%)	Silt (%)	Sand (%)	TOC (%)	Total N (%)	Total S (%)	Salinity (psu)	$SO_4^{=}/Cl^-$
Ucides cordatus site								
0–10	35.0	47.8	17.2	0.91	0.14	0.18	2.3	0.01
10–20	36.2	46.0	17.7	0.83	0.13	0.16	4.5	0.08
20–30	30.1	47.4	22.5	0.70	0.11	0.15	3.5	0.26
30–40	32.3	55.3	12.4	1.43	0.11	0.16	20.5	0.07
Uca maracoani site								
0–10	16.5	21.7	61.8	1.68	0.11	0.40	2.7	0.13
10–20	17.1	27.1	55.8	1.71	0.11	0.46	5.0	0.01
20–30	16.8	19.9	63.3	1.59	0.08	0.40	7.5	0.18
30–40	6.7	10.1	83.1	1.31	0.08	0.41	12.0	0.21
Control site								
0–10	25.9	30.1	44.0	2.91	0.21	0.41	n.d.	n.d.
10–20	13.6	26.2	60.2	2.30	0.17	0.28	n.d.	n.d.
20–30	37.7	50.7	11.7	1.58	0.13	0.14	n.d.	n.d.
30–40	13.9	19.8	66.3	1.97	0.16	0.27	n.d.	n.d.

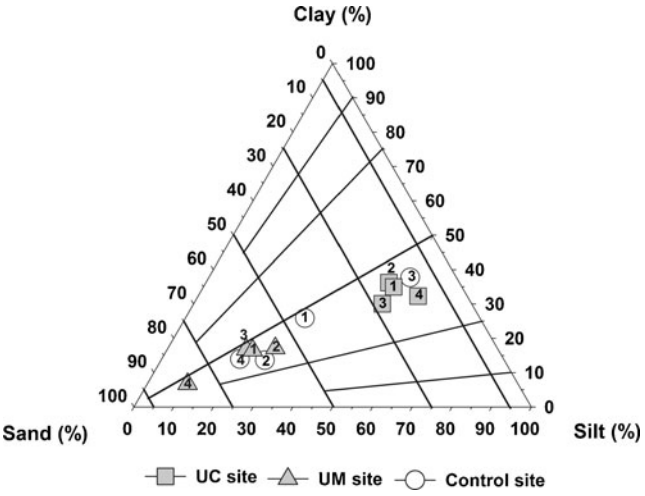

Fig. 3 Ternary diagram showing the distribution of sand, silt and clay at the different study sites and depths (*1* 0–10, *2* 10–20, *3* 20–30, and *4* 30–40 cm), according to the classification scheme proposed by Flemming (2000)

the total S values range from 0.14 to 0.41% at the control site (non-bioturbated).

pH, redox potential, salinity, and dissolved sulfate and chlorite

The pH varies significantly ($p<0.01$) between the bioturbated areas. However, depth-related differences are less pronounced. The lowest pH values were recorded at the UC site, where the values vary from 6.9 to 7.4 (Fig. 4). At the UM site, the pH values are higher and vary between 7.8 and 8.1. The pH levels of the soil at the control site are intermediate, ranging from 7.1 to 7.3. Some important physicochemical differences are also observed between the different soils types. As regards the redox potential at both bioturbated sites, Eh values are consistently positive and higher than those recorded at the control site (Fig. 4), indicating more oxidizing conditions. At the bioturbated sites, the highest Eh values are observed at the UC site, ranging between +29 and +218 mV, whereas lower Eh values are observed at the UM site (+12 to +68 mV). The lowest Eh values occur at the control site; this site is characterized by more reducing conditions in all down-core layers (Eh< 0 mV), values ranging from −50 to −30 mV (Fig. 4). As regards depth-related variations at the bioturbated sites, the redox potential decreases from the uppermost layers (0–20 cm) to the deeper layers (30–40 cm), whereas at the control site the Eh values vary little with depth.

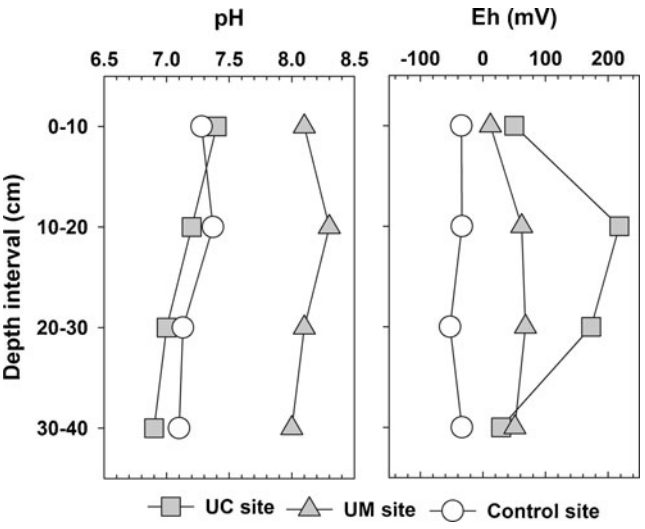

Fig. 4 Down-core trends of pH and Eh values at the three study sites

Salinity and dissolved anions (SO_4^{2-} and Cl^-) were measured only at the bioturbated sites, because of sampling difficulties. However, no significant differences were observed between the sites (Table 1). Pore water salinity remained between 2 and 7 psu within the upper layers at both sites, showing little differences between sites. Similarly, at both the UC and UM sites, the salinity values increase to 20 and 12 psu in deeper layers, respectively. Molar ratios of SO_4^{2-}/Cl^- in the pore water remained higher than in seawater (0.05) for most layers of both sites (except in $UC_{0–10\ cm}$ and $UM_{10–20\ cm}$).

Fractionation of Fe and degree of pyritization (DOP)

The sequential extraction of Fe differs clearly between the sites with *U. cordatus* and *U. maracoani* (Figs. 5, 6). The contents of exchangeable Fe (mean value for all of the samples: 0.54±0.26 μmol kg^{-1}) and Fe carbonate (6.5±4.8 μmol kg^{-1}) were always low, generally representing low free Fe contents ($\sum F1_{Fe} \rightarrow F6_{Fe}$), and were therefore not considered further in this study (Fig. 5). The highest contents ($p<0.05$) of reactive-Fe ($\sum F1 \rightarrow F5$) and Fe-oxyhydroxides ($\sum F3 \rightarrow F5$) are found at the UC site (mean values for all depths: reactive-Fe=168.65±28.63 and oxyhydroxides-Fe=163.35±28.45 μmol g^{-1}; Fig. 6). Intermediate contents (mean values for all depths) of reactive-Fe (85.85±14.03 μmol g^{-1}) and Fe-oxyhydroxides (78.82±14.32 μmol g^{-1}) are found at the UM site, whereas the lowest contents are observed at the non-bioturbated site (reactive-Fe=62.40±33.79 and Fe-oxyhydroxides=55.93±27.73 μmol g^{-1}). The contents of reactive-Fe and Fe-oxyhydroxides do not show any clear trends, and no differences are observed between layers (0–10, 10–20, 20–30, and 30–40 cm) at the bioturbated sites (Fig. 6).

Conversely, the highest Fe-pyrite contents (mean value for all depths; Figs. 5, 6) are observed at the control site (56.22±30.16 μmol g^{-1}), followed by the UM and then the UC site (16.02±5.98 and 13.52±16.75 μmol g^{-1}, respectively). As in the case of reactive-Fe and Fe-oxyhydroxides, there are no clear depth-related differences, with the exception

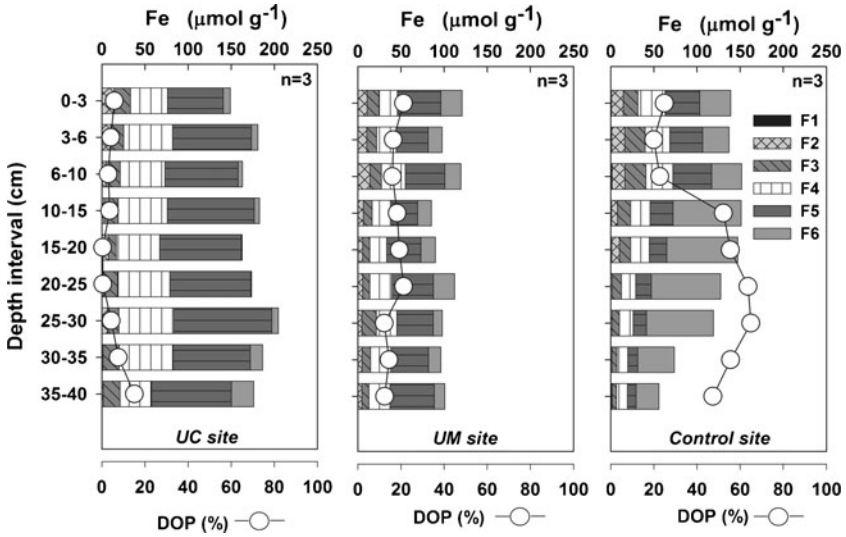

Fig. 5 Down-core trends of iron speciation and the degree of iron pyritization (DOP) at the three study sites. *F1* Exchangeable iron, *F2* carbonate-associated iron, *F3* ferrihydrite iron, *F4* lepidocrocite iron, *F5* crystalline oxides and iron oxyhydroxides, *F6* Fe-pyrite

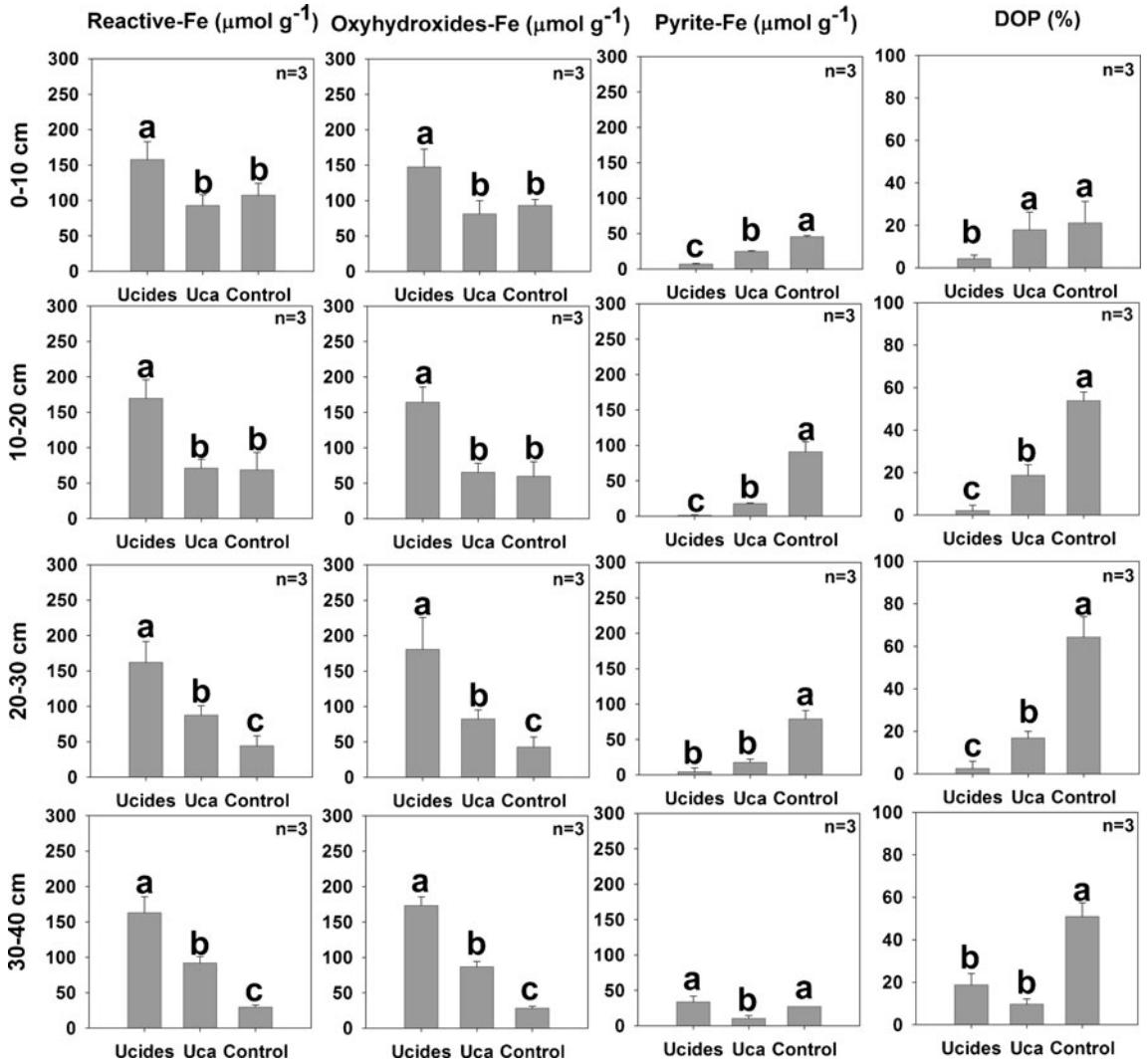

Fig. 6 Mean values (±standard deviation, $n=3$) of different forms of iron and the degree of iron pyritization (DOP) in all down-core soil layers of the three study sites. Bars with different letters indicate significant differences at $p<0.05$

of the UC site where the Fe-pyrite content increases in the deepest layer (30–40 cm, 39.47±11.64 μmol g^{-1}; Fig. 6).

The DOP values are consistent with those of Fe-pyrite, i.e., the highest values are found at the control site (mean value for all depths=47.92±17.76%; Figs. 5, 6), followed by the UM (15.76±5.76%) and the UC site (5.37±6.79%). At both bioturbated sites, the Fe-oxyhydroxide contents are significantly higher than those of the other forms of iron, accounting for approx. 90% of the total iron at the UC and 77% at the UM site. At the non-bioturbated site (control), in contrast, Fe-pyrite is the dominant form of iron at most depths, corresponding to approx. 56% of the total iron, except in the uppermost layer (0–10 cm, 24%; Fig. 6).

Discussion

Effects of crab activity on the composition and properties of mangrove soils

Previous studies have shown that the burrowing activity of crabs affects the physicochemical conditions of mangrove soils by downward translocation and exchange of gases via their burrows in response to the increased substrate–air/water interface area (Kristensen and Alongi 2006; Kristensen 2008). Thus, bioturbation may generate redox conditions favorable to iron respiration fuelled by oxidation of iron sulfides (Kristensen et al. 2000, 2010; Nielsen et al. 2003; Ferreira et al. 2007a; Ferreira 2010. Accordingly, the redox conditions at both bioturbated sites of the present study are mainly suboxic (Eh~100 mV), whereas anoxic (Eh< 50 mV) conditions prevail in all layers at the control site (Fig. 4). Thus, both species increase the aeration of the soils relative to the control (non-bioturbated) site. Although the burrow density is lower (12±3 m^{-2}) at the UC site, the soil is more oxidized than that at the UM site (58±12 burrows m^{-2}). This may be explained by differences in the width of the carapace of the two crab species (Fig. 2). Thus, in Brazilian mangroves, *Ucides cordatus* reaches larger maximum carapace sizes (male carapace width >90 mm, females >70 mm; Diele and Koch 2010), and also makes wider and deeper burrows (depth >210 cm; Schories et al. 2003) than *Uca maracoani* (depth ~40 cm; Lim 2006). The burrowing characteristics of *U. cordatus* imply the removal of a larger amount of sediment, which probably results in greater aeration at depth.

At both bioturbated sites the salinity of the interstitial water in all samples was found to be lower than that of the ambient seawater (31–34 psu; Table 1). This may be explained by the fact that the physiographic conditions at both sites are almost identical (location ~6 m from the estuary channel, similar elevation). As a consequence, both sites are exposed to similar tidal flooding periods. The somewhat higher salinities in the lowermost layers relative to the layers above may be related to the fact that sampling was carried out during the rainy season, the increase in salinity with depth reflecting increasing dilution by rainwater toward the top (Marchand et al. 2004; Ferreira et al. 2010).

The lower soil TOC contents at both bioturbated sites relative to those of the control site (Table 1) are consistent with the above-mentioned oxidizing processes. The oxygen exposure caused by the burrows favors aerobic and suboxic pathways of carbon decomposition (such as Fe reduction; Kristensen and Alongi 2006), and therefore increased rates of carbon oxidation. This interpretation is consistent with the highly significant negative correlation between Eh and TOC ($r=-0.910$, $p<0.01$, $n=12$; Fig. 7). Total N is also significantly correlated with TOC ($r=0.727$, $p<0.05$), which indicates that most of the N is associated with organic matter. In contrast, total S is poorly correlated with TOC ($r=0.491$, $p>0.05$), suggesting that S is to a large part present as inorganic S (mainly pyrite) in these environments (Otero et al. 2009).

Another possible explanation for the lower organic carbon contents at the bioturbated sites may be related to the feeding activity of the crabs. Thus, several studies have shown that the large mangrove crab *U. cordatus* is one of the most important litter-consuming crabs in tropical mangroves (e.g., Koch and Wolff 2002; Schories et al. 2003; Nordhaus et al. 2006; Nordhaus and Wolff 2007). According to Nordhaus et al. (2006), *U. cordatus* consumes 84.2% of the leaf litter in the mangroves along the NE coast of Brazil. Similarly, Schories et al. (2003) found that 61% of the leaf litter in the mangrove forests of northern Brazil was removed/consumed by this species. Since consumption and digestion of leaves occur simultaneously, this crab species is capable of feeding more or less continuously without any diurnal or tide-related feeding periodicity, which results in elevated levels of food consumption (Nordhaus et al. 2006). Moreover, other studies have shown that daily leaf

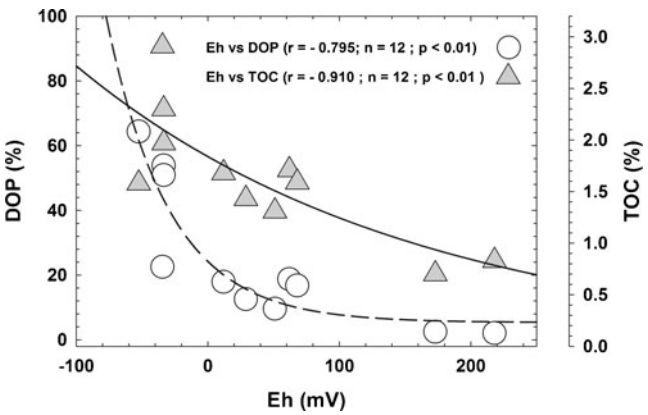

Fig. 7 Correlations between Eh, total organic carbon (TOC), and the degree of iron pyritization (DOP)

consumption per crab may be equal to or exceed the daily litter fall (Schories et al. 2003; Nordhaus et al. 2006).

In addition to leaf consumption and removal, leaf processing by crabs (through shredding and mastication) greatly enhances litter degradation (by providing suitable substrates for bacterial decomposition) in comparison with microbial decay alone, and thereby facilitates higher carbon mineralization in bioturbated mangrove forests (Koch and Wolff 2002; Nordhaus and Wolff 2007). On the other hand, fiddler crabs (*Uca* sp.) are considered important consumers of organic compounds supplied by primary production by microalgae and bacteria (Bouillon et al. 2002; Cannicci et al. 2008). The feeding activity of fiddler crabs involves scraping of the soil surface with their minor chelipeds, followed by a progressive production of small pseudo-pellets of processed substrate (Bartolini et al. 2009).

Effects of bioturbation on Fe and S geochemistry

Aeration of the soil by bioturbation will lead to oxidation of Fe sulfides with concomitant production of acidity and SO_4^{2-} (reactions 1 and 2 below), thus explaining the significantly lower pH values (Fig. 4) recorded at the UC site ($p<0.05$), as well as the excess sulfate found in all soil layers of the UC and UM sites (mean molar ratio $SO_4^{=}/Cl^-$ for all depths: UC=0.108±0.112 and UM=0.132±0.088; Table 1):

$$FeS_2 + H_2O + 7/2O_2 \rightarrow Fe^{2+} + 2SO_4^{2-} + 2H^+ \quad (1)$$

$$FeS + 3/2O_2 + H_2O \rightarrow Fe^{2+} + SO_4^{2-} + 2H^+ \quad (2)$$

The molar ratio of seawater is 0.05, low ratios (SO_4/Cl <0.05) indicating that the sulfate is being reduced, whereas higher ratios ($SO_4^{=}/Cl^-$ >0.05) indicate that the Fe sulfides are being oxidized (Giblin 1988). In addition, the oxidation process is also consistent with the significantly ($p<0.001$) higher Fe-oxyhydroxide contents in the soils of the two bioturbated sites (Figs. 5, 6) relative to the control site (mean values for all samples: bioturbated sites=118.77± 50.37, control=62.78±28.28). The Fe^{2+} produced by oxidation of the iron sulfides (reactions 1 and 2) may fuel precipitation of iron oxyhydroxides (according to reaction 3) by migration to layers where more oxidizing conditions predominate (Clark et al. 1998):

$$2Fe^{2+} + 1/2O_2 + 3H_2O \rightarrow 2FeOOH + 4H^+ \quad (3)$$

In fact, studies carried out under controlled conditions have shown that the Fe released by the oxidation of iron sulfides may hydrolyze to form amorphous ferric oxyhydroxides (Zhang and Evangelou 1996). According to Caetano et al. (1997), an increase in the pH of pore water during high tide due to the buffering effect of seawater favors the precipitation of soluble Fe as Fe-oxyhydroxides. The latter authors emphasize that Fe precipitation can take place rapidly (within 7 minutes after inundation of the soil by seawater). The oxidizing effect of crab burrowing activity on iron sulfides and the subsequent formation of iron oxides have also been observed in mangrove studies in southern Brazil (e.g., Ferreira et al. 2007a; Ferreira 2010).

Another aspect that must be taken into account is that the lower reactive-Fe and Fe-oxyhydroxide contents found at the UM site (Figs. 5, 6) are consistent with the sandier nature of the sediment at this site (see Fig. 3), which is probably related to higher energy conditions at the time of sedimentation (e.g., Molinaroli et al. 2009). In fact, the soil at the UM site is composed of muddy sand and slightly muddy sand, where the mud content decreases from 38% in the uppermost section (0–10 cm) to 17% in the lowermost one (30–40 cm; Fig. 3). The soil at the UC site, in contrast, consists of slightly sandy mud, with mud contents ranging from 78% (20–30 cm) to 88% (30–40 cm). Interestingly, the silt/clay ratio on average remains at a constant 1.5 (60:40) at both sites and all depths, whereas sand contents differ between sites. This indicates that, although the hydrodynamic energy conditions are higher at the UM site (higher sand content), the composition of the suspended matter is identical to that at the UC site (cf. Flemming 2000; Molinaroli et al. 2009).

However, although the highest free Fe contents found in the UC soil may be related to the finer grain size in comparison to the other two sites (see Fig. 3), the sequential extraction data (Figs. 5, 6) support the hypothesis that this is most probably due to oxidation of iron sulfides. The highest Fe-pyrite and DOP contents found at the control site, along with the low Eh (Fig. 4) and Fe-oxyhydroxide contents (Figs. 5, 6), are consistent with the interpretation that crab burrows have an oxidative effect on iron sulfides. In fact, for all analyzed samples, the Fe-pyrite contents at the control site are 3–6 times higher than those found at the UC and UM sites. Similarly, DOP values calculated for the non-bioturbated

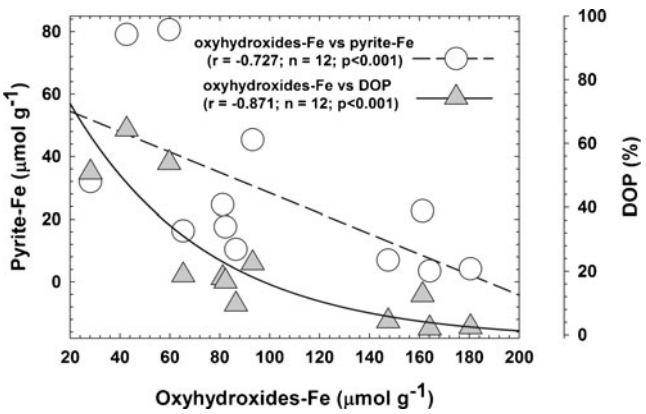

Fig. 8 Correlations between Fe-oxyhydroxides, Fe-pyrite, and the degree of iron pyritization (DOP)

site are 3–9 times higher than those calculated for the UC and UM sites (Figs. 5, 6). The differences between sites with and without crabs suggest that pyrite oxidation occurs mainly as a result of the burrowing activity of crabs.

This pyrite oxidation process will also cause a decrease in pH values (especially in UC; Fig. 4) and an excess of sulfate (Table 1), which is consistent with the enhanced formation of Fe-oxyhydroxides observed at the bioturbated sites (Figs. 5, 6). The negative and highly significant correlations between Fe-oxyhydroxides and Fe-pyrite, and between Fe-oxyhydroxides and DOP (Fig. 8), are consistent with the coupling between pyrite oxidation and the formation of iron oxyhydroxides. As the oxidation of pyrite involves the release of Fe^{2+}, it is possible that, at the UC and UM sites, Fe^{2+} is rapidly oxidized under pH conditions close to neutral, which is characteristic of tidally influenced systems (Otero and Macías 2002b; Otero et al. 2009). Thus, the substantial enrichment in Fe-oxyhydroxides observed in the bioturbated soils reveals the oxidative effect of burrowing by both crabs. On the basis of the increased Fe-oxyhydroxide contents and the extremely low DOP values in the bioturbated soils (ranging from 2.48 to 18.75%; Figs. 5, 6), crab burrowing activity appears to limit sulfate reduction and favor other carbon oxidation pathways (aerobic respiration and/or iron reduction). These data are consistent with the results of previous work in mangrove forests and salt marshes (Gribsholt et al. 2003; Nielsen et al. 2003; Kristensen et al. 2010), as well as with the significant negative correlation between Eh and DOP values in the present study ($r=-0.783$, $p<0.01$, $n=12$; Fig. 7).

Another important aspect is that the DOP values for the UC site are significantly lower than the corresponding values of the site populated by *U. maracoani* (Figs. 5, 6). This suggests that *U. cordatus* may exert a more intense oxidizing effect on mangrove soils than does *U. maracoani*. The differences in the impacts exerted by the two crabs are probably related to the larger body size (and therefore wider burrows) of *U. cordatus*, and also to the deeper burrows constructed by this species.

Conclusions

The results of the present study have demonstrated that:

- the burrowing activity of *Ucides cordatus* and *Uca maracoani* may considerably alter the composition, physicochemical properties, and geochemical conditions of semiarid mangrove soils, and the two species act in similar ways that favor aeration and oxidation of the soil;
- the oxidizing effects of crab burrows lead to pyrite oxidation, and thereby enhance the formation of iron oxyhydroxides in bioturbated soils; under these conditions, sulfate reduction is probably being suppressed by different carbon oxidation pathways (aerobic and Fe reduction); on the other hand, anaerobic conditions prevail in non-bioturbated soils, with a clear dominance of Fe-pyrite in the solid fraction and sulfate reduction as the main carbon oxidation process;
- the activity of *U. cordatus* has a higher oxidizing capacity than that of *U. maracoani*, probably because of the construction of larger burrows (both in length and diameter); although the impact of *U. maracoani* burrows on soil geochemical conditions is less pronounced, both crabs are important bioturbators in Brazilian mangrove systems, capable of enhancing and also evidently shifting the dominant pathway of organic matter decomposition;
- by implication, the impacts of burrowing crabs on the geochemistry of mangrove soils must be taken into consideration in environmental studies (e.g., trace metal bioavailability and mobilization, carbon dynamics), with special attention to species-specific effects.

Acknowledgements The first author benefited from a scholarship from Fundação Cearense de Apoio ao Desenvolvimento Científico e Tecnológico, FUNCAP. We thank Carmen Pérez Llaguno for laboratory assistance. We also appreciate constructive comments by three anonymous reviewers and the journal editors.

References

Alongi DM (2008) Mangrove forests: resilience, protection from tsunamis, and responses to global climate change. Estuar Coast Shelf Sci 76:1–13

Alongi DM, Tirendi F, Goldrick A (1996) Organic matter oxidation and sediment chemistry in mixed terrigenous-carbonate sands of Ningaloo Reef. West Aust Mar Chem 54:203–219

Alongi DM, Wattayakorn G, Pfitzner J, Tirendi F, Zagorskis I, Brunskill GJ, Davidson A, Clough BF (2001) Organic carbon accumulation and metabolic pathways in sediments of mangrove forests in southern Thailand. Mar Geol 179:85–103

Bacon JR, Davidson CM (2008) Is there a future for sequential chemical extraction? Analyst 133:25–46

Bartolini F, Penha-Lopes G, Limbu S, Paula J, Cannicci S (2009) Behavioural responses of the mangrove fiddler crabs (*Uca annulipes* and *U. inversa*) to urban sewage loadings: results of a mesocosm approach. Mar Pollut Bull 58:1860–1867

Berner RA (1970) Sedimentary pyrite formation. Am J Sci 268:1–23

Bianchini A, Lauer MM, Nery LEM, Colares EP, Monserrat JM, Filho EAS (2008) Biochemical and physiological adaptations in the estuarine crab *Neohelice granulata* during salinity acclimation. Comp Biochem Physiol 151:423–436

Botto F, Iribarne O (2000) Contrasting effects of two burrowing crabs (*Chasmagnathus granulata* and *Uca uruguayensis*) on sediment composition and transport in estuarine environments. Estuar Coast Shelf Sci 51:141–151

Bouillon S, Koedam N, Raman AV, Dehairs F (2002) Primary producers sustaining macro-invertebrate communities in intertidal mangrove forests. Oecologia 130:441–448

Bright DB, Hogue CL (1972) A synopsis of the burrowing land crabs of the world and list of their arthropod symbionts and burrow associates. Natural History Museum, Los Angeles

Caetano M, Falcao M, Vale C, Bebianno MJ (1997) Tidal flushing of ammonium, iron and manganese from intertidal sediment pore water. Mar Chem 58:203–211

Cannicci S, Burrows D, Fratini S, Smith TJ III, Offenberg J, Dahdouh-Guebas F (2008) Faunal impact on vegetation structure and ecosystem function in mangrove forests: a review. Aquat Bot 8:186–200

Castilho-Westphal GG, Ostrensky A, Pie MR, Boeger WA (2008) The state of the art of the research on the mangrove land crab, *Ucides cordatus*. Arch Vet Sci 13:151–166

Claff SR, Sullivan LA, Burton ED, Bush RT (2010) A sequential extraction procedure for acid sulfate soils: partitioning of iron. Geoderma 155:224–230

Clark MW, McConchie D, Lewis DW, Saenger P (1998) Redox stratification and heavy metal partitioning in *Avicennia*-dominated mangrove sediments: a geochemical model. Chem Geol 149:147–171

Clough BF (1992) Primary productivity and growth of mangrove forests. In: Robertson AI, Alongi DM (eds) Coastal and estuarine studies: tropical mangrove ecosystems. American Geophysical Union, Washington, DC, pp 225–250

Diele K, Koch V (2010) Growth and mortality of the exploited mangrove crab *Ucides cordatus* (Ucididae) in N-Brazil. J Exp Mar Biol Ecol 395:171–180

Diele K, Simith DJB (2006) Salinity tolerance of northern Brazilian mangrove crab larvae, *Ucides cordatus* (Ocypodidae): necessity for larval export? Estuar Coast Shelf Sci 68:600–608

Diele K, Koch V, Saint-Paul U (2005) Population structure, catch composition and CPUE of the artisanally harvested mangrove crab *Ucides cordatus* (Ocypodidae) in the Caeté estuary, North Brazil: indications for overfishing? Aquat Living Resour 18:169–178

EMBRAPA (1997) Manual de métodos de análise de solo. Empresa Brasileira de Pesquisa Agropecuaria, Centro Nacional de Pesquisa de Solos, Rio de Janeiro

FAO (2006) World reference base for soil resources: a framework for international classification, correlation and communication. United Nations Food and Agriculture Organization, Rome, World Soil Resources Report

Ferreira TO (2010) Bioturbation and its role in iron and sulfur geochemistry in mangrove soils. In: Otero XL, Macías F (eds) Biogeochemistry and pedogenetic process in saltmarsh and mangrove systems. Nova Science, New York, pp 183–205

Ferreira TO, Otero XL, Vidal Torrado P, Macías F (2007a) Effects of bioturbation by root and crab activity on iron and sulfur biogeochemistry in mangrove substrate. Geoderma 142:36–46

Ferreira TO, Otero XL, Vidal Torrado P, Macías F (2007b) Redox processes in mangrove soils under Rhizophora mangle in relation to different environmental condition. Soil Sci Soc Am J 71:484–491

Ferreira TO, Otero XL, Souza Junior VS, Vidal-Torrado P, Macías F, Firme LP (2010) Spatial patterns of soil attributes and components in a mangrove system in Southeast Brazil (São Paulo). J Soils Sediments 10:995–1006

Flemming BW (2000) A revised textural classification of gravel-free muddy sediments on the basis of ternary diagrams. Cont Shelf Res 20:1125–1137

Folhes MT, Rennó CD, Soares JV (2009) Remote sensing for irrigation water management in the semi-arid Northeast of Brazil. Agr Water Manag 96:1398–1408

Fortín D, Leppard GG, Tessier A (1993) Characteristic of lacustrine diagenetic iron oxyhydroxides. Geochim Cosmochim Acta 57:4391–4404

Gee GW, Bauder JW (1986) Particle-size analysis. In: Klute A (ed) Methods of soil analysis. Part 1. Physical and mineralogical methods. American Society of Agronomy and Soil Science, Madison, pp 383–412

Giblin A (1988) Pyrite formation in marshes during early diagenesis. Geomicrobiol J 6:77–97

Glaser M, Diele K (2004) Asymmetric outcomes: assessing central aspects of the biological, economic and social sustainability of a mangrove crab fishery, *Ucides cordatus* (Ocypodidae), in North Brazil. Ecol Econ 49:361–373

Gleason SM, Ewel KC, Hue N (2003) Soil redox conditions and plant-soil relationships in a Micronesian mangrove forest. Estuar Coast Shelf Sci 56:1065–1074

Gribsholt B, Kostka JE, Kristensen E (2003) Impact of fiddler crabs and plant roots on sediment biogeochemistry in a Georgia saltmarsh. Mar Ecol Prog Ser 259:237–251

Huerta-Díaz MA, Morse JW (1990) A quantitative method for determination of trace metal concentrations in sedimentary pyrite. Mar Chem 29:119–114

Huerta-Díaz MA, Morse JW (1992) Pyritization of trace metals in anoxic marine sediments. Geochim Cosmochim Acta 56:2681–2702

Hullebusch ED, Utomo S, Zandvoort MH, Lens PNL (2005) Comparison of three sequential extraction procedures to describe metal fractionation in anaerobic granular sludges. Talanta 65:549–558

Kathiresan K, Rajendran N (2005) Coastal mangrove forests mitigated tsunami. Estuar Coast Shelf Sci 65:601–606

Koch V, Wolff M (2002) Energy budget and ecological role of mangrove epibenthos in the Caeté estuary, North Brazil. Mar Ecol Prog Ser 228:119–130

Kostka JE, Roychoudhury A, van Cappellen P (2002) Rates and controls of anaerobic microbial respiration across spatial and temporal gradients in saltmarsh. Biogeochemistry 60:49–76

Kottek M, Griesser J, Beck C, Rudolf B, Bubel F (2006) World map of the Köppen-Geiger climate classification updated. Meteorol Zeitschr 15:259–263

Kristensen E (2008) Mangrove crabs as ecosystem engineers: with emphasis on sediment processes. J Sea Res 59:30–43

Kristensen E, Alongi DM (2006) Control by fiddler crabs (*Uca vocans*) and plant roots (*Avicennia marina*) on carbon, iron and sulfur biogeochemistry in mangrove sediment. Limnol Oceanogr 51:1557–1571

Kristensen E, Andersen FO, Holmboe N, Holmer M, Thongtham N (2000) Carbon and nitrogen mineralization in sediments of the Bangrong mangrove area, Phuket, Thailand. Aquat Microbial Ecol 22:199–213

Kristensen E, Mangion P, Tang M, Flindt MR, Holmer M, Ulomi S (2010) Microbial carbon oxidation rates and pathways in sediments of two Tanzanian mangrove forests. Biogeochemistry 102:231–245

Lim SSL (2006) Fiddler crab burrow morphology: how do burrow dimensions and bioturbative activities compare in sympatric populations of *Uca vocans* (Linnaeus, 1758) and *U. annulipes* (H. Milne Edwards, 1837)? Crustaceana 79:525–540

Machado W, Moscatelli M, Rezende LG, Lacerda LD (2002) Mercury, zinc, and copper accumulation in mangrove sediments surrounding a large landfill in southeast Brazil. Environ Pollut 120:455–461

Machado W, Carvalho MF, Santelli RE, Maddock JEL (2004) Reactive sulfides relationship with metals in sediments from an eutrophicated estuary in Southeast Brazil. Mar Pollut Bull 49:89–92

Marchand C, Baltzer F, Lallier-Vergès E, Albéric P (2004) Pore-water chemistry in mangrove sediments: relationship with

species composition and developmental stages (French Guiana). Mar Geol 208:361–381
Molinaroli E, Guerzoni S, De Falco G, Saretta A, Cucco A, Como S, Simeone S, Perilli A, Magni P (2009) Relationships between hydrodynamic parameters and grain size in two contrasting transitional environments: the Lagoons of Venice and Cabras, Italy. Sediment Geol 219:196–207
Morse JW (1994) Interactions of trace metals with authigenic sulfide minerals: implications for their bioavailability. Mar Chem 46:1–6
Neue HU, Gaunt JL, Wang ZP, Becker-Heidmann P, Quijano C (1997) Carbon in tropical wetlands. Geoderma 79:163–185
Nielsen OI, Kristensen E, Macintosh DJ (2003) Impact of fiddler crabs (*Uca* spp.) on rates and pathways of benthic mineralization in deposited mangrove shrimp pond waste. J Exp Mar Biol Ecol 289:59–81
Nordhaus I, Wolff M (2007) Feeding ecology of the mangrove crab *Ucides cordatus* (Ocypodidae): food choice, food quality and assimilation efficiency. Mar Biol 51:1665–1681
Nordhaus I, Wolff M, Diele K (2006) Litter processing and population food intake of the mangrove crab *Ucides cordatus* in a high intertidal forest in northern Brazil. Estuar Coast Shelf Sci 67:239–250
Otero XL, Macías F (2002a) Variation with depth and season in metal sulfides in salt marsh soils. Biogeochemistry 61:247–268
Otero XL, Macías F (2002b) Spatial and seasonal variation in heavy metals in interstitial water of salt marsh soil. Environ Pollut 120:183–190
Otero XL, Macías F (2003) Spatial variation in pyritization of trace metals in salt marsh soils. Biogeochemistry 62:59–86
Otero XL, Ferreira TO, Vidal-Torrado P, Macías P (2006) Spatial variation in pore water geochemistry in a mangrove system (Pai Matos island, Cananeia-Brazil). Appl Geochem 21:2171–2186
Otero XL, Ferreira TO, Huerta-Díaz MA, Partiti CSM, Souza V Jr, Vidal-Torrado P, Macías F (2009) Geochemistry of iron and manganese in soils and sediments of a mangrove system, Island of Pai Matos (Cananeia—SP, Brazil). Geoderma 148:318–335
Peel MC, Finlayson BL, McMahon TA (2007) Updated world map of the Köppen-Geiger climate classification. Hydrol Earth Sys Sci 11:1633–1644
Penha-Lopes G, Kristensen E, Flindt M, Mangion P, Bouillon S, Paula J (2010) The role of biogenic structures on the biogeochemical functioning of mangrove constructed wetlands sediments: a mesocosm approach. Mar Pollut Bull 60:560–572
Perillo GME, Minkoff DR, Piccolo MC (2005) Novel mechanism of stream formation in coastal wetlands by crab–fish–groundwater interaction. Geo-Mar Lett 25:214–220. doi:10.1007/s00367-005-0209-2
Ponnamperuma FN (1972) The chemistry of submerged soil. Adv Agron 24:29–96
Rome MS, Young-Williams AC, Davis GR, Hines AH (2005) Linking temperature and salinity tolerance to winter mortality of Chesapeake Bay blue crabs (*Callinectes sapidus*). J Exp Mar Biol Ecol 319:129–145
Schories D, Barletta-Bergan A, Barletta M, Krumme U, Mehlig U, Rademaker V (2003) The keystone role of leaf-removing crabs in mangrove forests of North Brazil. Wetl Ecol Manag 11:243–255
Seybold C, Mersie W, Huang J, McNamee C (2002) Soil redox, pH, temperature, and water-table pattern of a freshwater tidal wetland. Wetlands 22:149–158
Soil Survey Staff (2010) Keys to Soil Taxonomy, 11th edn. United States Department of Agriculture, Natural Resources Conservation Service, US Gov Print Office, Washington
Systat (2008) SigmaPlot for Windows Version 11.0. Systat Software Inc, Chicago
Tanaka MO, Maia RC (2006) Shell morphological variation of *Littoraria angulifera* among and within mangroves in NE Brazil. Hydrobiology 559:193–202
Tessier A, Campbell PGC, Bisson M (1979) Sequencial extraction procedure for the speciation of particulate trace metals. Anal Chem 51:844–855
Walters BB, Rönnbäck P, Kovacs JM, Crona B, Hussain SA, Badola R, Primavera JH, Barbier E, Dahdouh-Guebas F (2008) Ethnobiology, socio-economics and management of mangrove forests: a review. Aquat Bot 89:220–236
Zhang YL, Evangelou VP (1996) Influence of iron oxide forming conditions on pyrite oxidation. Soil Sci 161:852–864